Published in final edited form as:
Respir Physiol Neurobiol. 2008 May 31; 161(3): 273–280.

Monotone Signal Segments Analysis as a novel method of breath detection and breath-to-breath interval analysis in rat

Tijana Bojic[3], **Jasna Saponjic**[1*], **Miodrag Radulovacki**[4], **David W. Carley**[5], and **Aleksandar Kalauzi**[2*]

1*Department of Neurobiology, Institute for Biological Research Sinisa Stankovic, University of Belgrade, 11060, Belgrade, Serbia*

2*Department of Biophysics, Neuroscience and Biomedical Engineering, Institute for Multidisciplinary Research, 11000 Belgrade, Serbia*

3*School of Medicine, University of Belgrade, 11000 Belgrade, Serbia*

4*Department of Pharmacology, University of Illinois, Chicago, IL 60612, USA*

5*Center for Narcolepsy, Sleep and Health Research, University of Illinois, Chicago, IL 60612, USA.*

Abstract

We applied a novel approach to respiratory waveform analysis - Monotone Signal Segments Analysis (MSSA) on 6-h recordings of respiratory signals in rats. To validate MSSA as a respiratory signal analysis tool we tested it by detecting: breaths and breath-to-breath intervals; by detecting respiratory timing and volume modes; and by detecting changes in respiratory pattern caused by lesions of monoaminergic systems in rats.

MSSA differentiated three respiratory timing (tachypneic, eupneic, bradypneic-apneic), and three volume (artifacts, normovolemic, hypervolemic-sighs) modes. Lesion-induced respiratory pattern modulation was visible as shifts in the distributions of monotone signal segment amplitudes, and of breath-to-breath intervals. Specifically, noradrenergic lesion induced an increase in mean volume ($p \leq 0.03$), with no change of the mean breath-to-breath interval duration ($p \geq 0.06$). MSSA of timing modes detected noradrenergic lesion-induced interdependent changes in the balance of eupneic (decrease; $p \leq 0.02$), and tachypneic (an increase; $p \leq 0.02$) breath intervals with respect to control. In terms of breath durations within each timing mode, there was a tendency toward prolongation of the eupneic ($p \leq 0.08$) and bradypneic-apneic ($p \leq 0.06$) intervals. These results demonstrate that MSSA is sensitive to subtle shifts in respiratory rhythmogenesis not detectable by simple respiratory pattern descriptive statistics. MSSA represents a potentially valuable new tool for investigations of respiratory pattern control.

*Corresponding authors **Jasna Saponjic, M.D.,Ph.D.**, Research Associate Professor, Department of Neurobiology, Institute for Biological Research-Sinisa Stankovic, University of Belgrade, Despot Stefan Blvd. 142, 11060 Belgrade, Serbia, Phone: +381 11 2078426, Fax: +381 11 2761433, e-mail: jasnasap@ibiss.bg.ac.yu, **Aleksandar Kalauzi, Ph.D.**, Senior Scientist, Department of Biophysics, Neuroscience and Biomedical Engineering, Institute for Multidisciplinary Research, Kneza Viseslava 1a, 11000 Belgrade, Serbia, Phone: +381 11 2078465, Fax: +381 11 2761433, e-mail: kalauzi@ibiss.bg.ac.yu.

Keywords

monotone signal segments analysis; breath detection; breath-to-breath interval; rat; respiratory pattern modulation; monoaminergic lesion

1. Introduction

In order to assess basic properties of respiratory generators and accompanying modulatory systems, respiratory signals have been analyzed by a variety of analytical methods (Longobardo et al., 1982; Carley, 1989; Carley et al., 1989; Khoo, 1999; Saponjic et al., 2003). Two approaches appear as the most frequent: linear (such as Fourier, wavelet and correlation analysis techniques), and nonlinear. While linear methods can depict periodicity of respiratory patterns (Siegelova and Kopecny, 1985; Benchetrit, 2000), nonlinear methods (Hughson et al., 1995) enable analysis of different time-scaling characteristics. However, breath volumes and breath-to-breath (BB) intervals were not widely studied as random variables, though their corresponding probability distribution profiles could offer an additional and independent insight into the operation of relevant physiological systems. One of the possible approaches to achieve this is the extraction of monotone segments from the respiratory signal and thereby characterizations of the respiratory signal basic properties as relevant random variables.

Monotone Signal Segments Analysis (MSSA) has previously been employed as a tool to measure changes in neuronal unit (Jankovic, 2000; Todorovic et al., 2007) or neuronal population activity (Todorovic et al., 2007). A similar methodological approach was used for the analysis of linear decreases and increases of arterial blood pressure and pulse interval (Bertinieri, 1988; Zoccoli et al., 2001; Parati et al., 2006). The basic concept behind this approach is to observe any one dimensional signal as the series of monotone segments between two local extremums. In fact, in any such signal, continuous or discrete, one can locate an alternating series of maximums and minimums.

In this study we applied Monotone Signal Segments Analysis (MSSA) on 6-h recordings of respiratory signals in rats. We validated MSSA by detecting the breaths and BB intervals, by differentiating the distinct timing modes of the BB intervals in control recordings and their changes following monoaminergic system lesion-induced respiratory pattern modulation.

Materials and Methods

2.1 Operative procedure and recording

Experiments were performed in nine chronically instrumented male adult Sprague-Dawley rats. We recorded sleep and breathing during baseline conditions, following sham injection (saline i.p. 1 ml/kg), and every week for 5 weeks following injection of a systemic neurotoxin (1ml/kg, i.p., see details below). Prior to surgery and consistently throughout the experimental protocol, animals were maintained on a 12-hour light-dark cycle, and were housed at 25°C with free access to food and water. Principles for the care and use of laboratory animals in research were strictly followed, as outlined by the Guide for Care and Use of Laboratory animals (National Academy of Sciences Press, Washington; 1996).

All details of the surgical procedures employed for electrode implantation and systemically (i.p.) induced monoaminergic lesions have been previously described (Saponjic et al., 2007). After a postoperative recovery period of 2 weeks, the experimental recording sessions began.

For respiratory measurements we employed bias-flow-ventilated whole-body plethysmographs (PLYUNIR/U, Buxco Electronics, Inc., Sharon, CT, USA). The bias flow of room air (2 L/min) was more than one order of magnitude greater than the alveolar ventilation of the rat, ensuring that no re-breathing occurred. The dimensions of the chamber were 15 cm wide × 25 cm long × 15 cm high, allowing the animal free movement within the space. A cable plugged onto the animal's connector and passed through a sealed port carried the bioelectric activity from the head. Access to water was provided by bottle passed through a pressure tight seal. Thermal fluctuations associated with tidal respiration induce changes in pressure within the plethysmograph, which, under appropriate conditions, are proportional to tidal volume (Epstein et al., 1980; Christon et al., 1996; Carley and Radulovacki, 1999; Horner, 2003). To minimize the influence of the thermal and convective transients in room pressure, the box pressure was referenced to a low-pass filtered (time constant of 5 s) version of itself. In this way, low-frequency trends or drift in box pressure represented common-mode signals and were rejected by the differential pressure transducer (Model DP45-14; Validyne Engineering, Nothridge, CA). To minimize any possible artifact related to asymmetry or nonuniformity of pressure within the rectangular chamber, the transducer was mounted to and centered on the lid of the plethysmorgaph. Before any recording session the rats were individually adapted overnight in the small chamber space of the plethysmograph in which they were recorded. It was previously observed that this is a sufficient adaptation to the recording apparatus for adult rats, and that all of the measures relevant to the present study remain stable after this adaptation (Carley et al., 1997). All experimental recordings began at 9:00 and lasted 6 h. Each rat was always recorded in the same plethysmograph during all 8 occasions: baseline recording, after saline injection (sham control), and 6 times after injection of the toxin: first after 24 hours, and then after 7, 14, 21, 28 and 35 days (Saponjic et al., 2007).

In this study for testing of Monotone Signal Segments Analysis in detection of the monoaminergic lesions induced respiratory pattern disturbance we used only sham control recordings and recordings made 28 days after the neurotoxins injections. To follow the changes in respiratory pattern between control and post-lesion conditions, each rat served as its own control.

2.2. Fundamentals of Monotone Signal Segments Analysis

While applying the MSSA analysis, we assume that the signal properties within any monotone segment hold less information than do the positions and values of the local extremums. Therefore, by extracting the positions and values of successive minimums and maximums, we substitute the signal samples with these new data, reducing memory requirements and accelerating the subsequent off-line analyses (particularly convenient for long term recordings). Furthermore, when low frequency oscillations exist (Fig. 1), or any other trend-like baseline instability, threshold methods for detecting high amplitude phenomena (such as spikes in neural recordings) have been proven as inferior to mss (monotone signal segments) analysis (Jankovic, 2000). By analogy, these benefits should also convey to the detection of regular breaths and sighs in long-term respiratory recordings.

In mathematical terms, one can distinguish positive and negative monotone segments (mss^{+} and mss^{-}, respectively), depending on whether they are located between a local minimum and maximum, or vice versa. Consequently, any signal could be described as a union:

$$s(t) = \bigcup_i \left(\mathrm{mss}_i^{+} \cup \mathrm{mss}_i^{-}\right) \quad \text{or} \quad s(t) = \bigcup_i \left(\mathrm{mss}_i^{-} \cup \mathrm{mss}_i^{+}\right),$$

depending on whether the signal starts with a positive or negative mss. Conventionally, we discard part of the signal situated between the first recorded sample and first detected local extremum, as we do not know its full segment properties. Further, if we denote with

$\left(t_i^{\max}, s_i^{\max}\right)$ or $\left(t_i^{\min}, s_i^{\min}\right)$ time occurrences, and signal values in its *i*th detected local maximum or minimum (respectively), three basic mss properties could be defined:

a) for mss^+

duration as $d(\text{mss}_i^+) = t_j^{\max} - t_i^{\min}$

height as $h(\text{mss}_i^+) = s_j^{\max} - s_i^{\min}$

and slope as $s(\text{mss}_i^+) = \text{arctg}\dfrac{s_j^{\max} - s_i^{\min}}{t_j^{\max} - t_i^{\min}}$

where $j = i$ if the signal starts with mss_1^+ or $j = i + 1$ if it starts with mss_1^-.

b) for mss^-

duration as $d(\text{mss}_i^-) = t_j^{\min} - t_i^{\max}$

height as $h(\text{mss}_i^-) = s_j^{\min} - s_i^{\max}$

and slope as $s(\text{mss}_i^-) = \text{arctg}\dfrac{s_j^{\min} - s_i^{\max}}{t_j^{\min} - t_i^{\max}}$

where $j = i$ if the signal starts with mss_1^- or $j = i + 1$ if it starts with mss_1^+. A typical part of a rat respiratory signal, with some characteristic mss points, is presented on Fig. 2. In this work we studied distributions only of mss heights (breath volumes), as well as distributions of the derived BB intervals.

3. Results

3.1 MSSA detection of the breaths and breath-to-breath intervals

In order to study basic statistical properties of monotone segment heights, in our previous work we constructed their respective occurrence histograms before and after an experimental intervention (Todorovic et al., 2007). Such a histogram is in fact the distribution of the number of detected mss, $N(h(mss^{+/-}))$, which have heights that fall between $h(mss^{+/-})$ and $h(mss^{+/-})+\delta h(mss^{+/-})$, where $\delta h(mss^{+/-})$ denotes the incremental histogram abscissa interval. In the case of the respiratory signals, examination of the modality of distribution of all mss^+ heights (Fig. 3A) enabled us to differentiate functional breathing inspiriums (breathing volumes) from artifacts (usually visible as small height mss^+ within the respiratory signal recorded by plethysmography). In Fig. 2. such a small height mss^+ could be seen between the second and third, but not between the first two inspiriums. The presence of these atrefacts makes the calculation of a BB interval, as a sum of durations of the negative and its following positive signal segment, impossible. In fact, irregularity of the artifacts appearance makes the construction of the distribution histograms of all mss^+ heights necessary. In addition, presence of sighs, as larger amplitude mss^+, could also be detected and quantified using the mss^+heights distribution histograms.

3.2 MSSA detection of respiratory volume modes

To operationalize this approach, it is necessary first to identify the most prominent, approximately normally distributed mode within a histogram, denoted as $N_b(h(mss^+))$ on Fig. 3A. In addition, small height mss^+ form a relatively narrow, sharp peak situated around $h(mss^+) \approx 0$ (N_a). The limit between N_b and N_a could easily be found as the minimum in the histogram profile (down arrow in Fig. 3A). On the other hand, the sighs, although present in

the signal, did not form a peak that would, with its shape, resemble N_b, but were rather sparsely distributed along the abscissa to the right side of N_b. Owing to the relatively greater number of normovolemic inspiriums with respect to the number of sighs, they became visible in the "tail" of histogram only after changing the scale of $N(h(mss^+))$ (Insert of Fig. 3A). However, by calculating the logarithm and square root of histogram values, an approximately normally distributed component (N_b) becomes linear, while mss heights belonging to hypervolemic breaths and sighs, since not normally distributed, leave the trend set by the right side of N_b. The result, shown on Fig. 4A, permits distinction of three, rather than two, respiratory volume components: N_a (low volume deflections which may be physiologic or artifactual), N_n (normovolemic), and N_{hs} (hypervolemic breaths and sighs).

3.3 MSSA detection of respiratory timing modes

A similar approach can be applied to the detection and characterization of respiratory timing modes. In mathematical terms, we introduce a new random variable, $(T_b)_i=(t_b)_{i+1}^{\max}-(t_b)_i^{\max}$, denoting temporal intervals between neighboring tidal inspiriums, or BB intervals (Fig. 2.), occurring at $(t_b)_i^{\max}$ and $(t_b)_{i+1}^{\max}$. The impact of different experimental conditions on respiratory pattern modulation could then be studied on respective distributions of $N(T_b)$, or number of BB intervals.

Observing $N(T_b)$ histograms obtained from the 6-h respiratory recordings, three main components of respiratory timing were observed in all nine experimental animals: a dominant central peak, consisting of regular eupneic inter-inspirium BB intervals $N_e(T_b)$; a smaller left tachypneic peak $N_t(T_b)$; and a number of bradypneic-apneic intervals, sparsely distributed, $N_{ba}(T_b)$ (Fig. 3B). Again, more detailed presence of N_{ba} intervals is depicted in the insert of Fig.3B.

In order to verify that the histogram components N_t, N_e and N_{ba} really consist of tachypneic, eupneic and bradypneic-apneic BB intervals, it was necessary to determine the limits between respective $N(T_b)$ components. Such a limit was easily noticed between N_t and N_e. However, between N_e and N_{ba} there was often no clear minimum in the histogram profile upon which to establish the limit. By calculating the logarithm and square root of histogram values, an approximately normally distributed component (N_e) becomes linear (Fig. 4B), while N_{ba} exhibits a nonlinear dependence, permitting a more exact determination of the component limits. Such a transformed histogram, of the same data previously shown on Fig. 3B, is presented in Fig. 4B.

In order to locate particular BB intervals belonging to individual components N_t, N_e and N_{ba}, a MATLAB program was developed by which we were able to identify and mark the respective BB intervals in the original time domain of respiratory signal. An example of such identification of the three types of intervals is presented on Fig. 5.

3.4 MSSA detection of the respiratory pattern modulation

To test our novel methodological approach in respiratory pattern modulation detection, we applied MSSA on 6-h recordings of respiration after systemically induced monoaminergic system lesions in rats from our former study (Saponjic et al, 2007), and compared the results between control and lesioned rats.

The effects of systemically (i.p.) induced monoaminergic efferent system lesions on respiratory pattern modulation were visible on both $N_b(h(mss^+))$ and $N(T_b)$ histograms by changing their positions (right shift, Fig. 6A1, Fig. 6B2), rather than altering their shapes, particularly following noradrenergic efferent system lesion.

In noradrenergic lesioned rats (by DSP-4 neurotoxin injection; n = 5), an increase in mean volume of breathing was observed 28 days after lesion (control: 289.76 ± 99.07 au; lesion: 397.84 ± 79.26; paired t-test: $t = -3.34$, $p \leq 0.03$), while there was no significant change of the mean values of BB interval duration (control: 0.71 ± 0.03 s; lesion: 0.77 ± 0.06 s; paired t-test: $t = -2.01$, $p \geq 0.06$).

By componential analysis of the BB intervals distribution we observed that all three breathing components (N_t, N_e and N_{ba}), specific for control animals, were also present 28 days after DSP-4 lesion. The mean values of the limits between N_t and N_e, and N_e and N_{ba} were not statistically different after the lesion (N_t/N_e control: 0.33 ± 0.02 s, N_t/N_e lesion: 0.34 ± 0.03 s; $t = -1.5$; $p \geq 0.10$; N_e/N_{ba} control: 1.16 ± 0.09 s, N_e/N_{ba} lesion: 1.29 ± 0.09 s; $t = -2.09$, $p \geq 0.05$). The lesion effects on the mean values of number and duration of BB intervals of separate $N(T_b)$ components, and on the mean volume, are illustrated in Table. 1.

The absolute number of eupneic intervals statistically decreased in DSP-4 lesioned rats ($t = 2.96$; $p \leq 0.04$), while the absolute number of tachypneic intervals showed a tendency to increase ($t = -2.35$, $p \geq 0.07$). By analyzing normalized values (obtained by dividing absolute number of intervals of a particular component with the total number of intervals) we confirmed this reciprocal interdependence of eupneic ($t = 3.56$, $p \leq 0.02$), and tachypneic number of intervals ($t = -3.77$; $p \leq 0.02$). A tendency to increase after the lesion was detected for eupneic and bradypneic-apneic BB interval duration (Table 1. ***t2***: $t = -2.38$, $p \leq 0.08$; ***t3***: $t = -2.35$, $p \leq 0.06$, respectively).

In serotonergic lesioned rats (by PCA neurotoxin injection; n = 4) no change in the mean value of breathing volume was observed (control: 287.63 ± 52.92 au; lesion: 329.08 ± 95.83; paired t-test, $t = -1.75$; $p \geq 0.09$), neither the change in the mean value of BB interval duration (control: 0.70 ± 0.10 s; lesion: 0.77 ± 0.05 s; paired t-test, $t = -1.94$; $p \geq 0.07$).

Also, 28 days after PCA lesion all three components of breathing intervals were present. Group mean values of the limits between N_t and N_e, and N_e and N_{ba} were not statistically different (N_t/N_e control: 0.34 ± 0.01 s, N_t/N_e lesion: 0.34 ± 0.02 s; $t = -0.21$; $p \geq 0.42$ N_e/N_{ba} control: 1.21 ± 0.05 s, N_e/N_{ba} lesion: 1.27 ± 0.10 s; $t = -1.26$: $p \geq 0.15$). Detailed results of the componential analysis are shown in Table 2. No significant changes were detected between values of control and lesioned animals.

3.5. Comparison between MSSA and the threshold crossing method

The threshold crossing method for breath detection is critically influenced by the threshold level, and this can be difficult to optimize. If the threshold is too low, artifactual deflections may be construed as physiological breaths. Conversely, a too-high threshold value would exclude some physiological, but hypovolemic breaths from detection. Therefore the objective determination of the threshold level is necessary, where the problem of determining its optimal value could be regarded analogous to the problem of finding the limit between N_a and N_b in Fig. 3A. The small amplitude deflections represented by N_a may arise from numerous sources including environmental disturbances to ambient pressure, motor movements of the animal and, most frequently, small oscillations in airway pressure due to cardiac contractions. These small deflections can be clearly seen during central apnea (Fig. 5C). In any case, the population of deflections characterized by N_a are “non-respiratory”. Therefore, finding the optimal threshold level for the threshold crossing technique should be based on constructing the histogram of respiratory local maxima values. In an ideal case, a bimodal profile should be expected — one mode originating from “artifacts”, the other from breaths. The optimal threshold level should be positioned in the minimum between these two modes.

In order to verify our new method we applied both MSSA and the threshold crossing technique to 14 control respiratory recordings. In 11 recordings the threshold crossing method produced the expected bimodal distribution of local maxima (Fig. 7A), while in 3 recordings tri-modal distributions were observed (Fig. 8). Bimodal distributions were typical for rats with stable respiratory baseline (insert of Fig. 7A), while tri-modal profiles occurred in the presence of trend-like changes in baseline (insert of Fig. 8). In contrast, by using MSSA bimodal distributions of mss+ heights were observed in all recordings (Fig. 7A; Fig.8). Therefore, with respect to the threshold crossing method, MSSA offers a more robust detection of physiological breaths, and their separation from the artifacts. Signals that present polymodal distributions of local maxima are a particular problem for the threshold approach (Fig. 8). In the case that bimodal distrubutions are developed by both MSSA and threshold crossing techniques, these methods yielded congruent detection of respiratory timing modes (Fig. 7 B).

Although not the subject of this work, it is clear that by using MSSA it is possible to calculate the durations and distributions of inspiriums directly as the difference between the local maximum and minimum positions of the corresponding monotone signal segments $d(\mathrm{mss}_i^+)=t_j^{\max}-t_i^{\min}$ (Fig.2.). Similarly, expiriums could be examined as the population of mss^- segments. As exemplified here, we obtained total breath time as the difference between maxima positions of two consecutive inspiriums. The same advantages noted above for MSSA versus threshold analysis would also pertain to future studies focused on respiratory phase detection and control.

4. Discussion

In this work we propose analysis of monotone signal segments as a novel methodological approach in respiratory signal analysis. To validate MSSA, we presented how MSSA detects breaths and BB intervals, how it defines classical respiratory pattern parameters (volume and timing modes), and how it detects modulation of respiratory pattern in terms of volume and timing modes.

MSSA is complementary to other linear and nonlinear methods of respiratory signal analysis, where respiratory parameters are accounted as temporal variables. It offers statistical distributions of breath volumes and BB intervals, revealing the distinct modes of both respiratory parameters. In addition, with MSSA an objective assessment of the modal limits is possible. The method is convenient particularly for long-term recordings. As demonstrated in section 2.3, we were able to detect changes in respiratory pattern in terms of both respiratory parameters following the lesions of monoaminergic system in rats.

The first work that analyzed the statistical distribution of respiratory parameters (tidal volume, inspiratory and expiratory time) was performed by Davis and Stagg, (Davis and Stagg, 1975). By analysis of a relatively small number of registered breaths (approx. 200) the authors concluded that the distributions of tidal volume, inspiratory and expiratory time were, in general, unimodal. The present study over a long-time scale refines this interpretation by presenting a systematic analysis of over 30,000 breaths per each rat (Table 1 and Table 2).

In biological systems multimodal distributions are commonly expressed by homeostatic control systems. Often, this phenomenon reflects the existence of multiple generating mechanisms (multiple sites of generation), or the multiple regimes of one generating mechanism (one site of generation). Decomposition of a multimodal distribution into its individual normal components provides insight into the underlying neural generating mechanisms. The multimodal distribution of BB intervals and its logarithmic transformation clearly evidenced three components; N_t, N_e and N_{ba}. In order to verify the type of respiratory pattern associated with each component, a MATLAB program was developed to mark the

respective BB intervals in the original time domain of the respiratory signal (Fig. 5). By determining the limits between individual components we were able to detect and quantify changes in each component induced by monoaminergic lesions. Analysis of these changes could further be an objective of other various basic and clinical studies.

Following noradrenergic lesion, a shift toward larger eupneic tidal volumes was observed, a finding that confirmed results of our previous study (Saponjic et al., 2007). Using modal analysis of the BB interval distribution we determined that all three respiratory timing components (N_t, N_e and N_{ba}) identified under control conditions remained present 28 days after DSP-4 injection, implying that the basic components of breathing rhythm were still present after noradrenergic lesion. The finding that the mean values of the limits between N_t and N_e and N_e and N_{ba} were not statistically different after DSP-4 lesion with respect to control condition, may indicate that the neural mechanisms generating the tachypneic, eupneic and bradypneic-apneic components of respiratory pattern continue to operate under the same regime despite the deficit in noradrenergic control of the ponto-medullary respiratory pattern generator.

While classical respiratory parameters analysis (Saponjic et al., 2007) did not find any change in the mean respiratory rate during any sleep/wake state in rats with noradrenergic system lesion, the MSSA uncovered the fine redistribution of respiratory pattern components, as a consequence of impaired noradrenergic neurotransmission. Specifically, the impact of this lesion was observed as a decreased number of eupneic and an increased number of tachypneic intervals. This result might suggest the predominant impact of tachypnea generating subregions of ventral respiratory group (Monnier et al., 2003) in respiratory pattern modulation. Alternatively, increased activity within the lateral parabrachial region or rostral Kölliker-Fuse nucleus may contribute to an increased propensity toward tachypneic patterns after noradrenergic lesion (Chamberlin and Saper, 1994). Simultaneously, in terms of the duration of certain BB intervals, there was a tendency for prolongation of eupneic and bradypneic/apneic intervals (Table 1).

In contrast, serotonergic lesion produced no changes in either the mean volume of breathing, or the mean BB interval duration, confirming the results from our previous study (Saponjic et al., 2007). As for noradrenergic lesions, all three components of the BB interval distribution remained intact and functioning within the same margins of the respiratory regime. Detailed analysis of the N_t, N_e and N_{ba} components in serotonergic lesion (Table 2) did not reveal any significant changes between control and post-lesion conditions. These data indicate that the serotonergic lesion might have milder effects on BB interval components with respect to the noradrenergic lesion. Although we previously demonstrated that the serotonergic lesion induced an increase in post-sigh sleep-apnea frequency and duration (Saponjic et al., 2007), here we did not specifically analyze sleep-related respiratory phenomena. For that purpose, future adaptations of the MSSA approach for distinction of post-sigh and spontaneous central apneas within N_{ba} component may yield new insights into the mechanisms of sleep related respiratory disturbances.

Although we presented here multimodal histograms of the respiratory mss^+ heights that differentiated functional breathing inspiriums from artifacts and physiologically augmented breaths (hypervolemic breaths and sighs) as shown in Fig. 3A and Fig. 4A, additional sophistication of the methodological approach is needed for volume-related automatic sigh detection and differentiation of spontaneous and sigh-related apneas. Analysis of monotone signal segments also offers a possibility to cross analyze different respiratory timing modes with particular respiratory volume modes to throw light on new aspects of the mechanisms of respiratory pattern modulation.

Acknowledgment

This work was supported by Serbian Ministry of Science and Environmental Protection Grants 143005, 143027, 145062 , and NIH Grant AG016303.

References

Benchetrit G. Breathing pattern in humans: diversity and individuality. Respir Physiol 2000;122:123–129. [PubMed: 10967339]

Bertinieri G, di Rienzo M, Cavalazzi A, Ferrari AU, Pedotti A, Mancia G. Evaluation of baroreceptor reflex by blood pressure monitoring in unanesthetized cats. Am J Physiol 1988;254:H377–H383. [PubMed: 3344828]

Carley, DW. Minimal modeling of hyman respiratory stability. In: Khoo, M., editor. Modeling and parameter estimation in respiratory control. NY: Plenum Press; 1989. p. 171-180.

Carley DW, Maayan C, Grimes J, Shannon DC. Breath-by-breath respiratory timing and volume control during periodic breathing. Am J Physiol 1989;257:R653–R660. [PubMed: 2782467]

Carley DW, Radulovacki M. Mirtazapine, a mixed-profile serotonin agonist/antagonist, suppresses sleep apnea in the rat. Am J Respir Crit Care Med 1999;160:1824–1829. [PubMed: 10588592]

Carley DW, Trbovic SM, Bozanich A, Radulovacki M. Cardiopulmonary control in sleeping Sprague-Dawley rats treated with hydralazine. J Appl Physiol 1997;83:1954–1961. [PubMed: 9390968]

Chamberlin NL, Saper CB. Topographic organization of respiratory responses to glutamate microstimulation of the parabrachial nucleus in the rat. J Neurosci 1994;14:6500–6510. [PubMed: 7965054]

Christon J, Carley DW, Monti D, Radulovacki M. Effects of inspired gas on sleep-related apnea in the rat. J Appl Physiol 1996;80:2102–2107. [PubMed: 8806919]

Davis JN, Stagg D. Interrelationships of the volume and time components of individual breaths in resting man. J Physiol 1975;245:481–498. [PubMed: 1142186]

Epstein RA, Epstein MA, Haddad GG, Mellins RB. Practical implementation of the barometric method for measurement of tidal volume. J Appl Physiol 1980;49:1107–1115. [PubMed: 7440298]

Horner, RL.; Stephenson, R.; O'Donnell, CP. Instrumentation and methods for chronic studies of sleep and breathing in rodents. In: Carley, DW.; Radulovacki, M., editors. Sleep-related breathing disorders. Experimental models and therapeutic potentials. New York, Basel: Marcel Dekker, Inc.; 2003. p. 19-55.

Hughson RL, Yamamoto Y, Fortrat JO. Is the pattern of breathing at rest chaotic? A test of the Lyapunov exponent. Adv Exp Med Biol 1995;393:15–19. [PubMed: 8629472]

Jankovic, B.; Kalauzi, A.; Culic, M.; Saponjic, J. Recognition and Separation of Simple and Complex Action Potentials of Purkinje Cells Using Personal Computer; Proceedings of the XLIV ETRAN Conference III; 2000. p. 223-226.

Khoo, M. Periodic breathing and central apnea. In: Altose, MD.; Kawakami, Y., editors. Control of Breathing in Health and Disease. Vol. 135. New-York-Basel: Marcel Dekker Inc; 1999. p. 203-250.

Longobardo GS, Gothe B, Goldman MD, Cherniack NS. Sleep apnea considered as a control system instability. Respir Physiol 1982;50:311–333. [PubMed: 6819618]

Monnier A, Alheid GF, McCrimmon DR. Defining ventral medullary respiratory compartments with a glutamate receptor agonist in the rat. J Physiol 2003;548:859–874. [PubMed: 12640009]

Parati G, Faini A, Valentini M. Blood pressure variability: its measurement and significance in hypertension. Curr Hypertens Rep 2006;8:199–204. [PubMed: 17147917]

Saponjic J, Radulovacki M, Carley DW. Respiratory pattern modulation by the pedunculopontine tegmental nucleus. Respir Physiol Neurobiol 2003;138:223–237. [PubMed: 14609512]

Saponjic J, Radulovacki M, Carley DW. Monoaminergic system lesions increase post-sigh respiratory pattern disturbance during sleep in rats. Physiol Behav 2007;90:1–10. [PubMed: 16989875]

Siegelova J, Kopecny J. Spectral analysis of breathing pattern in man. Physiol Bohemoslov 1985;34:321–331. [PubMed: 2932752]

Todorovic D, Kalauzi A, Prolic Z, Jovic M, Mutavdzic D. A method for detecting the effect of magnetic field on activity changes of neuronal populations of Morimus funereus (Coleoptera, Cerambycidae). Bioelectromagnetics 2007;28:238–241. [PubMed: 17203477]

Zoccoli G, Andreoli E, Bojic T, Cianci T, Franzini C, Predieri S, Lenzi P. Central and baroreflex control of heart rate during the wake-sleep cycle in rat. Sleep 2001;24:753–758. [PubMed: 11683478]

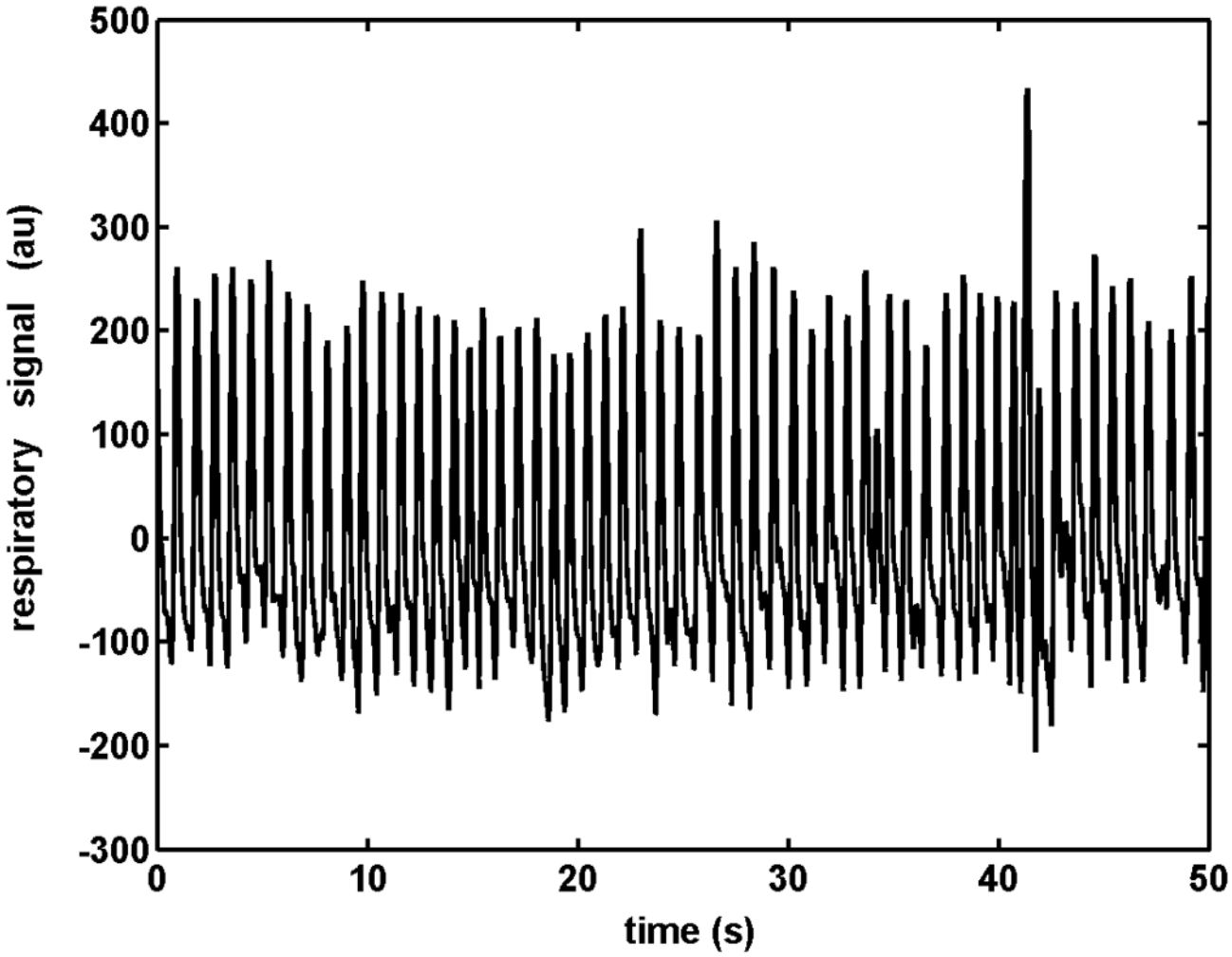

Fig. 1.

Respiratory signal, obtained as output from the plethysmograph, recorded from a rat following saline injection (control). The presence of low frequency oscillations can be visually appreciated. au - arbitrary units.

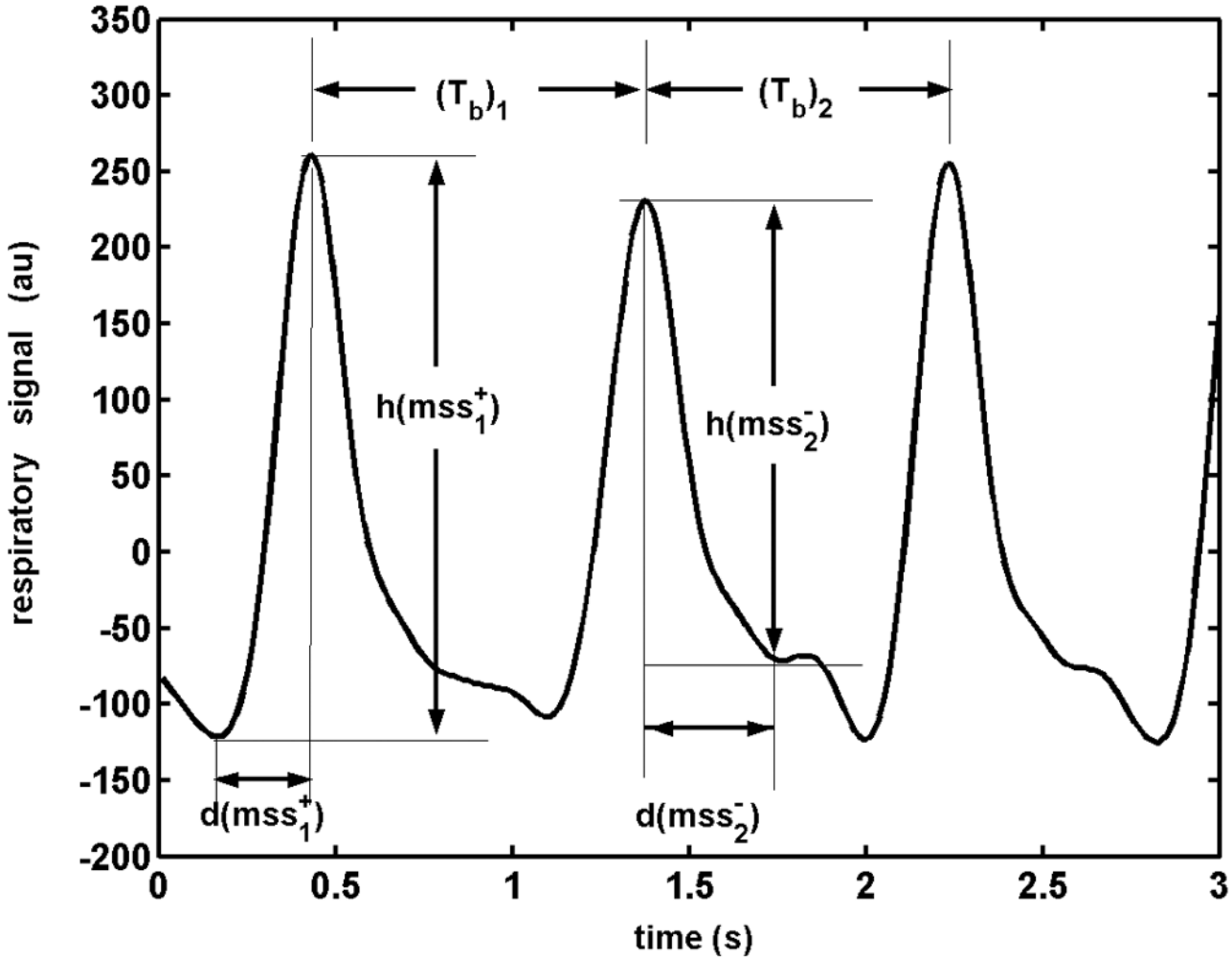

Fig. 2.

An expanded segment of the respiratory signal illustrated in Fig. 1, depicting the characteristic $mss^{+/-}$ (monotone signal segments) quantitative properties: $h(\mathrm{mss}_1^+)$,$h(\mathrm{mss}_2^-)$ - heights of the first positive and second negative mss, respectively; $d(\mathrm{mss}_1^+)$,$d(\mathrm{mss}_2^-)$ - durations of the respective mss; $(T_b)_1$, $(T_b)_2$ — breath-to-breath (BB) intervals; au - arbitrary units.

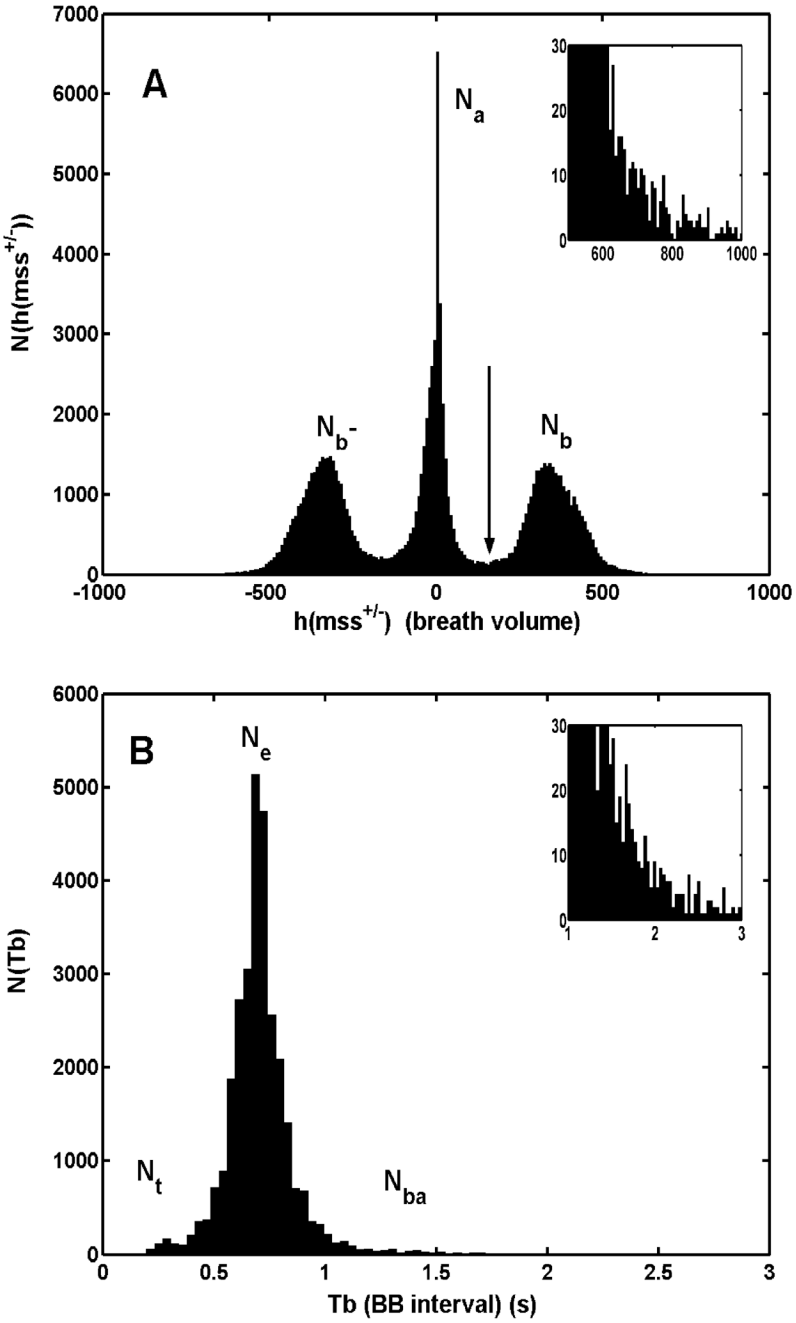

Fig. 3.

A. A typical distribution histogram presenting the number of monotone respiratory signal segments $N(h(mss^{+/-})$, distributed by their heights, during a 6 h of recording in rat under control conditions. Positive and negative breathing peaks, N_b and N_b-, and one formed by non-respiratory, artifactual small height mss, N_a, are marked separately. Limit between N_a and N_b is pointed by a down arrow. **Insert:** Magnified part of the right side of N_b, visualising the presence of sighs. **B.** Histogram of the number of BB intervals, $N(T_b)$, by their duration, T_b. Three modes within the respiratory pattern ($N(T_b)$) distribution are marked as: N_e (eupneic), N_t (tachypneic) and N_{ba} (bradypneic-apneic). **Insert:** Magnified part of N_{ba}, visualising the presence of bradypneic-apneic intervals.

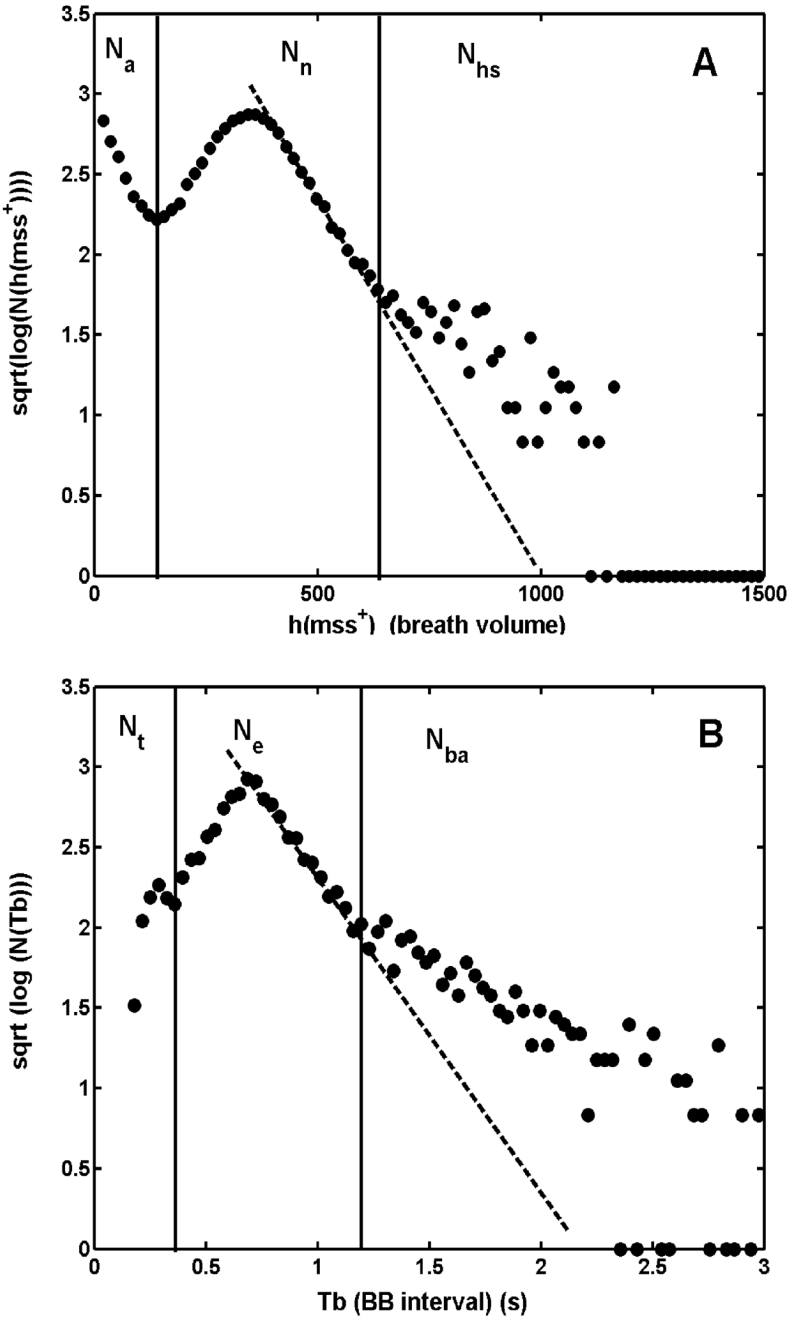

Fig. 4.

A. Distribution of the square root of logarithms of monotone signal segments numbers, sqrt (log(N(h(mss^+))), by their respective heights, h(mss^+). Three volume modes within this respiratory pattern distribution are marked as: N_a (artifacts), N_n (normovolemic) and N_{hs} (hypervolemic breaths and sighs). In the N_{hs} region, points leave the linear trend of N_n, indicated by a dashed line, positioned at the hypervolemic side of N_n (data from Fig. 3A). **B.** Distribution of the square root of logarithms of BB intervals numbers, sqrt(log(N(T_b))), by their respective interval durations, T_b (data from Fig. 3B). Three timing modes are marked as: N_t (tachypneic), N_e (eupneic) and N_{ba} (bradypneic-apneic). In the N_{ba} region, points leave the linear trend of N_e, indicated by a dashed line, positioned at the bradypneic side of N_e.

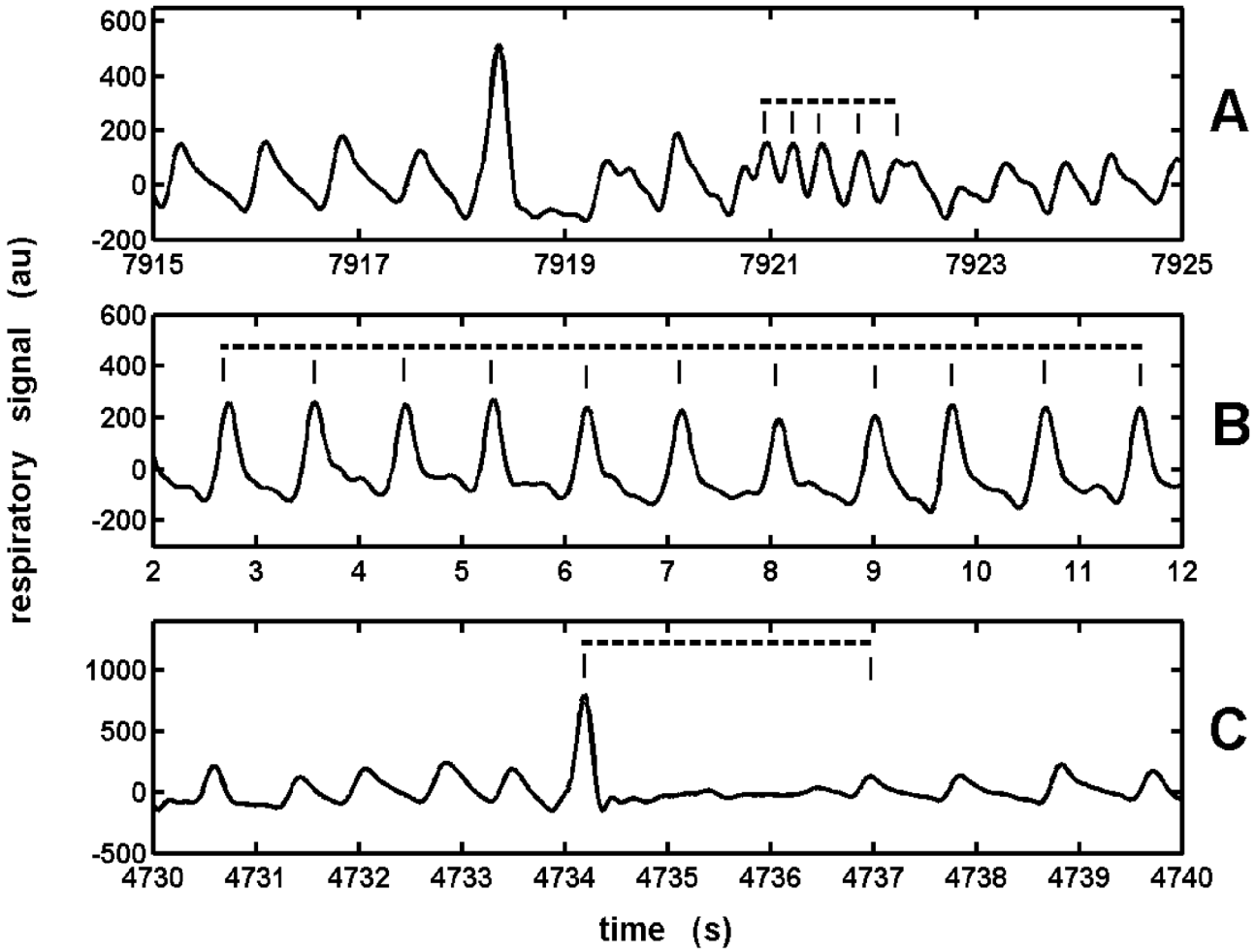

Fig. 5.

Examples of the verification results that histogram components N_t, N_e and N_{ba} from Fig. 4 consist of tachypneic (**A**), eupneic (**B**) and bradypneic-apneic (**C**) BB intervals, respectively. Identified intervals are marked by horizontal dashed lines. au -arbitrary units.

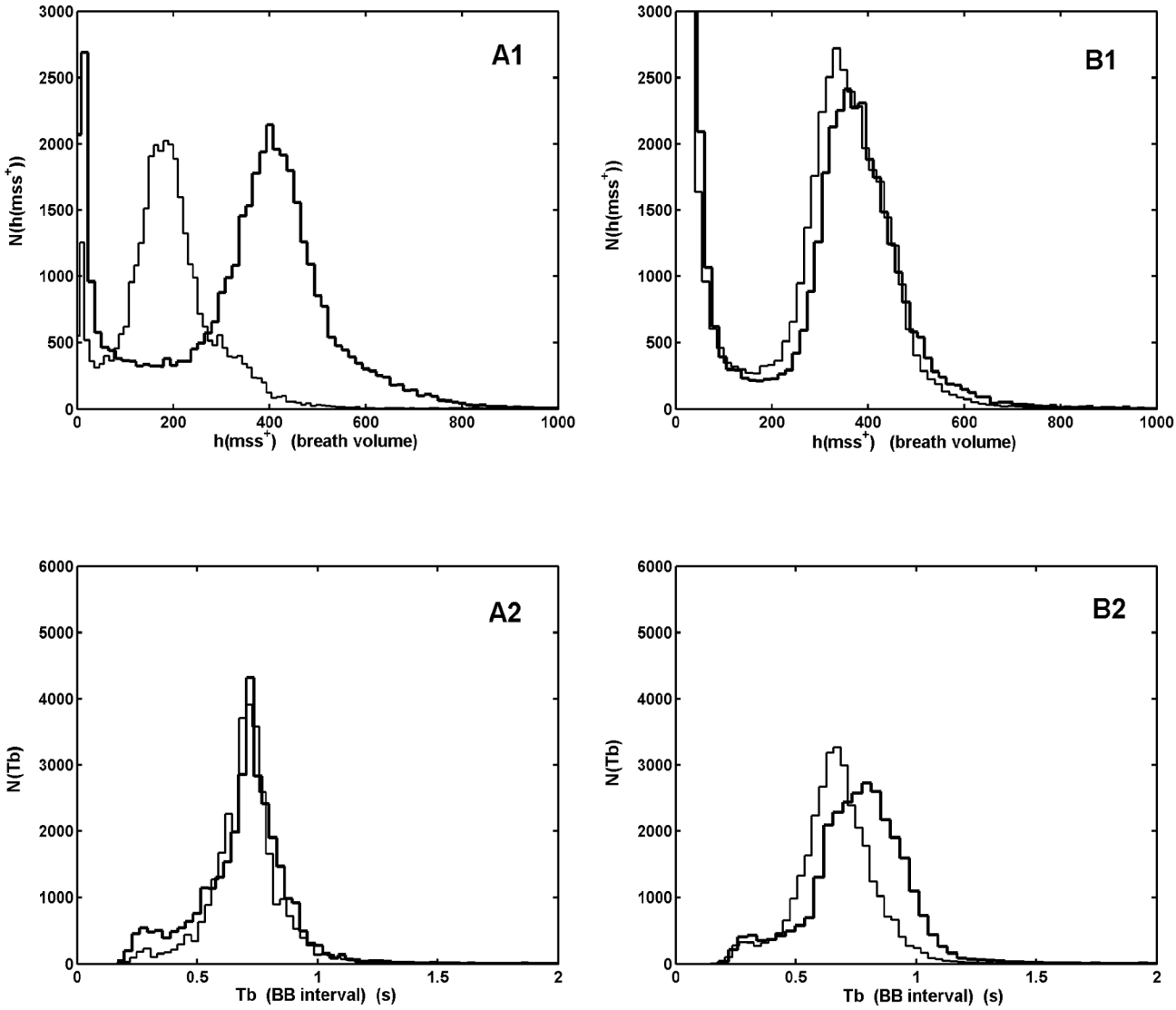

Fig. 6.

Example of the relationship between breathing volume and BB interval shifts in two noradrenergic lesioned animals (**A** and **B**). Greater shift in breathing volumes (**A1**) was coupled with no shift in BB intervals (**A2**); small shift in volumes (**B1**) was observed together with a greater shift in BB intervals (**B2**). Bold line — lesion, thin line — control.

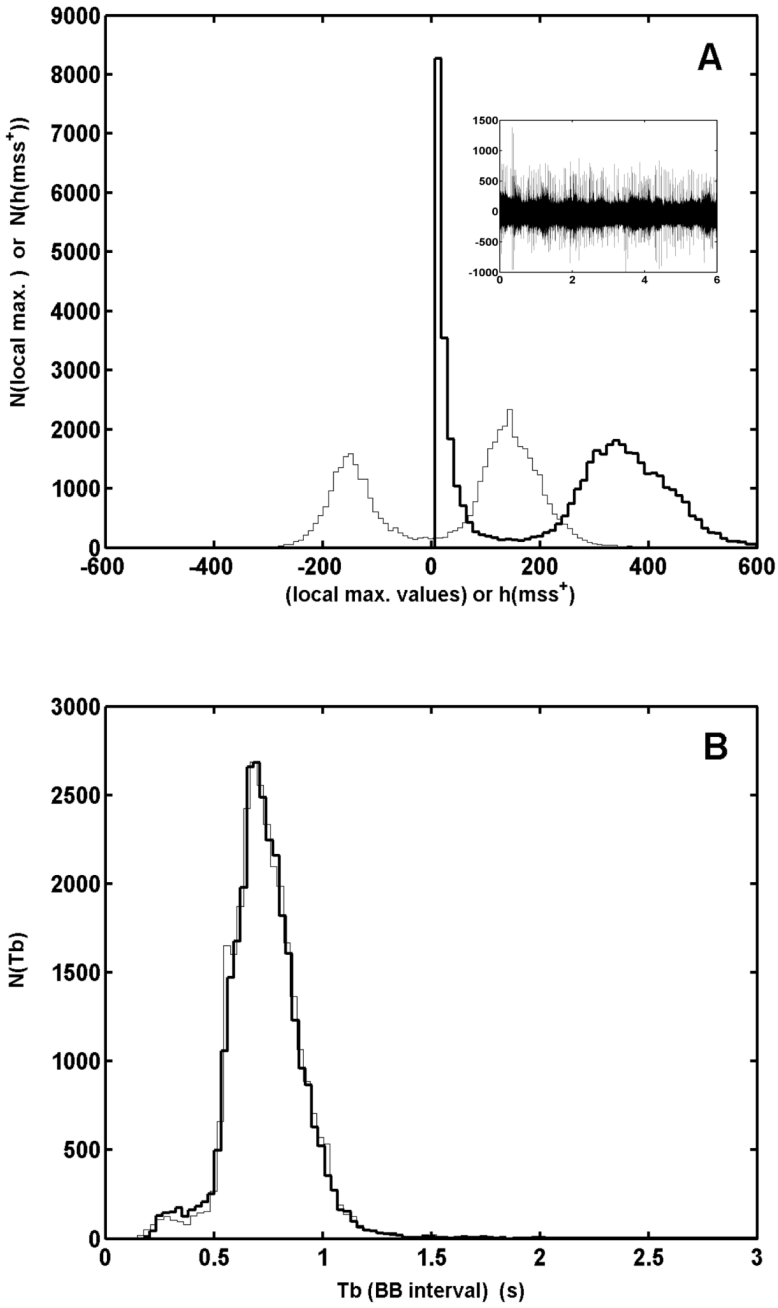

Fig. 7.

(A) Typical bimodal histograms of monotone respiratory signal segments $N(h(mss^{+}))$ heights (thick line); and local maximums by their values (thin line), in a case or stable respiratory baseline throughout a 6-h recording (insert). **(B)** Distributions of the number of BB intervals (N(Tb)) by their durations (Tb) obtained by MSSA (thick line) and by the threshold crossing method (thin line).

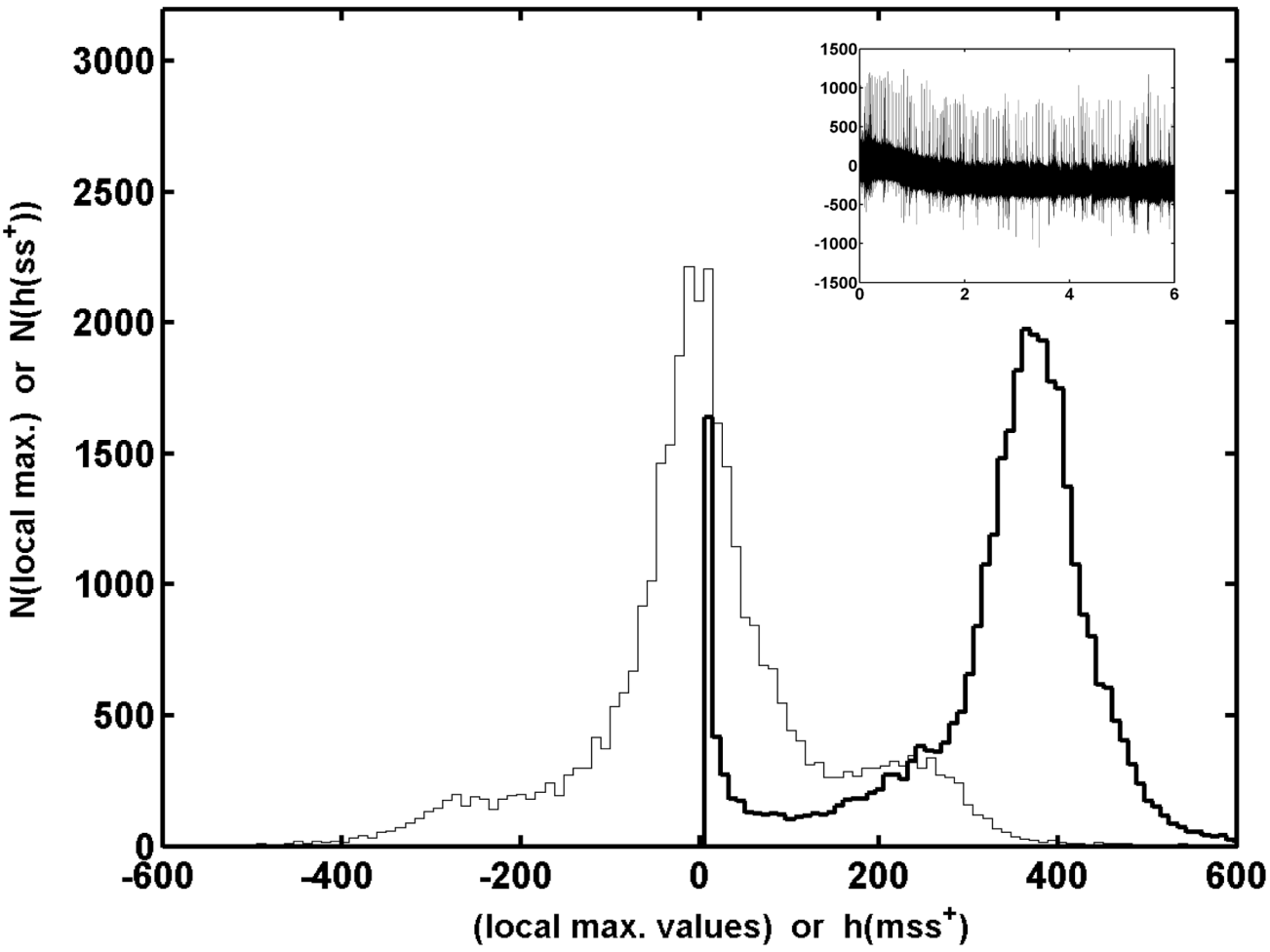

Fig. 8.

The bimodal histogram of monotone respiratory signal segments $N(h(mss^{+})$ by their heights (thick line); and the tri-modal histogram of local maximums by their values (thin line), in a case of unstable respiratory baseline during a 6-h recording (insert).

Table 1

Group mean values ± standard deviation of control vs. DSP-4 lesion values; number of BB intervals, BB interval duration, and breathing volume during 6 h of recordings.

DSP-4	Number of BB intervals		BB interval duration		Breathing volume	
	control	lesion	control	lesion	control	lesion
Tachypnea	A. 826.6 ± 337.0 N.**0.03**	A. 1262.0 ± 191.8 NS^{t1} N.**0.05** **	0.27 ± 0.01	0.27 ± 0.02 NS	**289.76 ± 99.07**	**397.84 ± 79.26** *
Eupnea	A.**29055.6 ± 1342.7** N.**0.96**	A.**26275.2 ± 2352.6** * N.**0.94** *	0.70 ± 0.02	0.77 ± 0.06 NS^{t2}		
Bradypnea/ Apnea	A.520.8 ±175.9 N.0.02	A.489.2 ±189.5 NS N.0.02 NS	1.584 ± 0.19	1.845 ± 0.14 NS^{t3}		
Total	30522.8 ±1313.6	28122.6 ±2456.7 NS	0.706 ±0.03	0.769 ±0.06 NS		

A - absolute number

N - normalized number.

* $p<0.05$

** $p<0.01$

NS, Non Significant

^{t1} tendency to increase ($p \leq 0.08$)

^{t2} tendency to increase ($p \leq 0.08$)

^{t3} tendency to increase ($p \leq 0.06$).

Table 2

Group mean values ± standard deviation of control vs. PCA lesion values: number of BB intervals, BB interval duration and breathing volume during 6 h of recording.

PCA	Number of BB intervals		BB interval duration		Breathing volume	
	control	lesion	control	lesion	control	lesion
Tachypnea	A. 1705.8 ± 811.2 N. 0.07	A. 1665.5 ± 672.7 NS N. 0.07 NS	0.269 ± 0.01	0.271 ± 0.01 NS	287.627 ± 52.92	329.084 ± 95.83 NS
Eupnea	A.28828.3 ± 3625.4 N. 0.93	A. 25914.8 ± 1881.7 NS N. 0.92 NS	0.712 ± 0.09	0.767 ± 0.05 NS		
Bradypnea/ Apnea	A. 459.8 ± 212.6 N. 0.02	A. 610.5 ± 257.6 NS N. 0.02 NS	1.78 ± 0.05	2.02 ± 0.28 NS		
Total	31119.3 ± 4052.7	28301.0 ± 1843.1 NS	0.704 ± 0.10	0.77 ± 0.05 NS		

A - absolute number

N - normalized number

NS - Non Significant - for paired t-test.